

M. KONIECZNY*, A. DZIADON[†]*

MECHANICAL BEHAVIOUR OF MULTILAYER METAL-INTERMETALLIC LAMINATE COMPOSITE SYNTHESISED BY REACTIVE SINTERING OF Cu/Ti FOILS

WŁASNOŚCI MECHANICZNE KOMPOZYTU WARSTWOWEGO METAL – FAZY MIĘDZYMETALICZNE UZYSKANEGO Z FOLII MIEDZIANEJ I TYTANOWEJ

Copper-intermetallic laminated composites have been fabricated through reactive sintering in vacuum using Cu sheets (0.7 mm thick) and Ti foils with different initial thickness (0.07, 0.1 and 0.12 mm). The titanium layers were completely consumed resulting in microstructures of well-bonded metal-intermetallic laminated composites with Cu residual metal layers alternating with the titanide intermetallic layers. The mechanical properties and fracture behaviour of the fabricated laminated composites were examined under different loading directions (perpendicular and parallel directions to laminate plane) through compression and impact tests. The results indicated that the composites exhibited anisotropic features. The strength in parallel compression was about 50% higher than in perpendicular compression. The specimens compressed in the parallel direction failed by cracking along the middle of the intermetallic layers, buckling of copper layers and cracking inclined $30\div 45^\circ$ to the interface initiating the formation of shear bands in the copper layers. The specimens compressed in the perpendicular direction failed by cracking of the intermetallic layers perpendicular to the interface. Cracking of intermetallic layers in turn involved shear deformation of the copper layers, which was localised in the spacing between opposite cracks. Impact tests showed that when the load perpendicular to the laminates was applied, the composites displayed superior impact toughness. The toughness increased with increasing remaining copper thickness. The failure during impact testing occurred by cleavage mode showing limited plastic deformation for the specimens loaded parallel to the laminates and extensive plastic deformation for the specimens loaded perpendicularly.

Keywords: metal-intermetallic laminated composite, mechanical behaviour, copper

Z blachy miedzianej i folii tytanowej ułożonych naprzemiennie w pakiet uzyskano na drodze wysokotemperaturowej syntezy faz międzymetalicznych kompozyt warstwowy. Grubość blachy miedzianej wynosiła 0,7 mm, a folii tytanowych: 0,07, 0,1 i 0,12 mm. W wyniku reakcji syntezy warstwy tytanu przereagowały całkowicie z częścią miedzi, tworząc z nie przereagowanymi do końca warstwami miedzi kompozyt miedź – fazy międzymetaliczne. Badano własności mechaniczne i mechanizm niszczenia uzyskanych kompozytów obciążanych w kierunku prostopadłym i równoległym do kierunku jego warstw. Przeprowadzono testy ściskania i udarności. Rezultaty badań wykazały iż kompozyt charakteryzuje się anizotropią własności. Próbki ściskane w kierunku równoległym do warstw miały o około 50% wyższą odporność na ściskanie niż obciążane prostopadłe do warstw. W kompozytach obciążanych równolegle do warstw następowało wzdłużne pękanie warstwy faz międzymetalicznych, rozszerzanie się pęknięć, a następnie wyginanie warstw miedzi. W przypadku kompozytu o najgrubszych warstwach faz międzymetalicznych, oprócz pęknięć wzdłużnych pojawiły się także pęknięcia na kierunkach występowania pasm ścinania nachylone pod kątem $30\div 45^\circ$ do osi próbki przechodzące zarówno przez warstwy miedzi jak i warstwy faz międzymetalicznych. W kompozytach obciążanych prostopadłe do warstw następowało plastyczne odkształcanie miedzi w kierunkach prostopadłych do kierunku ściskania oraz poprzeczne pękanie kruchych warstw faz międzymetalicznych pod wpływem naprężeń rozciągających te warstwy. Deformacja plastyczna warstw miedzi była blokowana przez związane z nimi warstwy faz międzymetalicznych a miedź mogła się odkształcać plastycznie tylko w małych obszarach pomiędzy pęknięciami w warstwach faz. Wyniki badania udarności próbek łamanych w dwóch prostopadłych do siebie kierunkach pokazały, że udarność próbek z karbem naciętym równolegle do warstw była przeszło dwukrotnie większa niż próbek z karbem naciętym przez wszystkie warstwy. Różnica ta wynikała z odmiennych mechanizmów niszczenia kompozytów. Udarność kompozytów wzrastała wraz ze wzrostem grubości warstw miedzi.

* KIELCE UNIVERSITY OF TECHNOLOGY, DEPARTMENT OF METALS SCIENCE AND MATERIALS TECHNOLOGIES, 25-314 KIELCE, AL. 1000-LECIA PP 7, POLAND

1. Introduction

Metal-intermetallic composites can be fabricated via many different techniques. They are known to be very attractive for a number of potential applications: electronic devices, armour and other structural components. As a distinct class of materials, intermetallics have good high-temperature strength, high resistance to corrosion and oxidation, high stiffness, good creep resistance and relatively low density. On the other hand, most intermetallics exhibit brittle fracture and low tensile ductility at room temperatures, because of limited dislocation mobility and insufficient number of slip or twinning systems resulting in little to no plastic deformation at the crack tip. Several composite reinforcement concepts involve material combinations consisting of one brittle and one ductile constituent. Examples include metal matrix composites and laminated composites comprised of alternate layers of intermetallics with metals. The intermetallic phases give high hardness and stiffness to the composite, while unreacted metal provides the necessary high strength, toughness and ductility for the system to concurrently be flexible. The multilayered structure of the composite allows for variations in the layer thickness and phase volume fractions of the components simply through the selection of initial thickness, which consequently allows for the optimisation of mechanical properties for practical applications. Methods for the production of laminated metal-intermetallic composites include magnetron sputtering [1–3], electron beam evaporation [4, 5] and synthesis reactions between dissimilar elemental metal foils. Earlier researches reveal that metal-intermetallic laminated composites can be produced by reaction synthesis that occurs at the interface of Ni and Al [6–13], Fe and Al [7, 14–16], Nb and Al [17–21], Mg and Al [22], Ti and Al [7, 8, 23–28] or Al and titanium alloy (Ti3Al2.5V or Ti6Al4V) [29, 30] foils. This technique has been also recently used to produce laminated composites using Cu and Ti foils [31–35]. Measurements have shown [31] that the composite consisting of copper layers partitioned by layers of intermetallics, offer very attractive combination of electrical conductivity and wear resistance. Designing laminar composites to obtain optimal mechanical properties requires knowledge of the composite failure mechanism. Previous works [7, 8, 19, 23, 26, 28, 29, 33, 34, 36–46] have investigated the mechanical and fracture properties of metal-intermetallic laminate composites, and proposed several models of crack propagation. The aim of this work is to study the mechanical properties and anisotropic features of copper-intermetallic laminated composites under different loading directions and volume fraction of constituents.

2. Experimental procedure

For metal-intermetallic laminated composites fabrication titanium foils were alternatively stacked between copper sheets of 0.7 mm thickness. Chemical composition and mechanical properties of used materials are shown in Table 1.

TABLE 1
Chemical composition and mechanical properties of foil materials

Material	Chemical composition, %	Mechanical properties
Copper	Cu: 99.99, Fe: 0.001, Ni: 0.001, Zn: 0.001, Sn: 0.001, Pb: 0.001, Sb: 0.001, As: 0.001, S: 0.001, Bi: 0.0001	Yield strength: 69MPa Ultimate strength: 218MPa Hardness: 72HV0.065
Titanium	Ti: 99.02, Fe: 0.09, C: 0.02, Al: 0.27, V: 0.09, Cr: 0.05, Mo: 0.01, O: 0.44, N: 0.01	Yield strength: 348MPa Ultimate strength: 459MPa Hardness: 220HV0.065

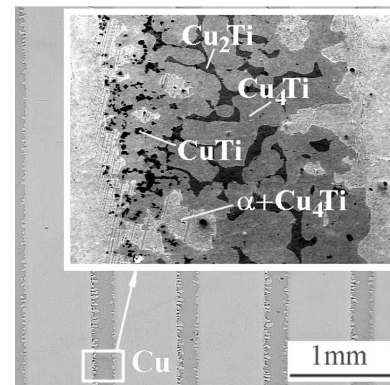


Fig. 1. Microstructure of the Cu-intermetallic phases laminated composite

The titanium foil thicknesses were initially selected (0.07, 0.1 and 0.12 mm thick) to completely consume the titanium in forming the intermetallic compounds with alternating layers of partially unreacted Cu metal. The dimensions of the processed samples-sandwiches were in the shape of platelets as 55 mm x 10 mm x 10 mm. The sandwiches were placed in a vacuum furnace. A pressure of 5 MPa that was used to ensure a good bonding between copper and titanium layers was released at temperature of 850°C. After holding at 890°C for 10 minutes the samples were furnace-cooled till room temperature. As a result of reaction with the liquid phase contribution all titanium has been fully consumed and transformed together with part of copper sheets into a structure composed of several intermetallic phases, analysed formerly [32], mainly: Cu₄Ti and also Cu₂Ti, CuTi and solid solution titanium in copper (α). Products of high temperature reactions assumed shape of the layers (Fig. 1).

Characteristics of Cu-intermetallic laminated composite materials

Starting foil thickness mm		Layers number		Final layer thickness mm		Volume fraction of unreacted copper in composite, %
Cu	Ti	Cu	Ti	d_{Cu}	D_i	
0.7	0.12	13	12	0.493	0.331	60
0.7	0.10	14	13	0.548	0.223	71
0.7	0.07	14	13	0.624	0.127	83

Detailed information concerning the synthesis of copper-intermetallic laminated composite has been published previously [31, 32]. The titanide phases give high hardness (510÷550 HV0.065 [31]) and stiffness to the composite, while unreacted copper provides the necessary high strength and ductility. The multilayered structure of the composite allows for variations in the layer thickness and phase volume fractions of the Cu and Ti components simply through the selection of initial thickness. Table 2 lists representative thickness value and layer number of starting foil, thickness of final metal and intermetallics and volume fraction of unreacted copper in fabricated composites.

The analysis of the above results indicates that the thicknesses of layers in the fabricated composites are related to the initial titanium foil thickness through the relationships:

$$d_{Cu} = 0.7 - \frac{d_{Ti}^2}{0.07} - \frac{d_{Ti}}{11} \quad (1)$$

$$d_i = \frac{d_{Ti}^2}{0.0728} + \frac{d_{Ti}}{1.168}, \quad (2)$$

where d_{Cu} is the thickness of unreacted copper layer in the composite, d_i is the thickness of intermetallics layer in the composite and d_{Ti} is the thickness of initial titanium foil.

The compression tests were conducted on cubic samples with dimension of 10 mm. Before straining the lateral walls of samples were carefully mechanically polished initially with a grade 800 abrasive paper and finally using Struers polishing machine, and subsequently etched. Etching was performed with solution of 40 g CrO_3 – 7.5 g NH_4Cl – 8 ml H_2SO_4 – 50 ml HNO_3 – 1900 ml H_2O to reveal the copper grain boundaries. Quasi-static compression tests were performed at a strain rate of $1.7 \cdot 10^{-3} s^{-1}$ on an Instron screw machine. The Charpy impact tests were conducted on rectangular samples with typical dimensions of 55 mm × 10 mm × 10 mm. The samples were notched using a low speed saw. V-notches were introduced at the centre part of the test bars perpendicular and parallel to the laminates. The mechanical tests were conducted in both perpendicular and

parallel directions to the metal-intermetallic interfaces for different volume fractions of copper (60%, 71% and 83%). Microstructural observations were performed using a JEOL JMS-5400 scanning electron microscope and a Carl Zeiss NEOPHOT 2 optical microscope. The crack location and crack orientation were investigated.

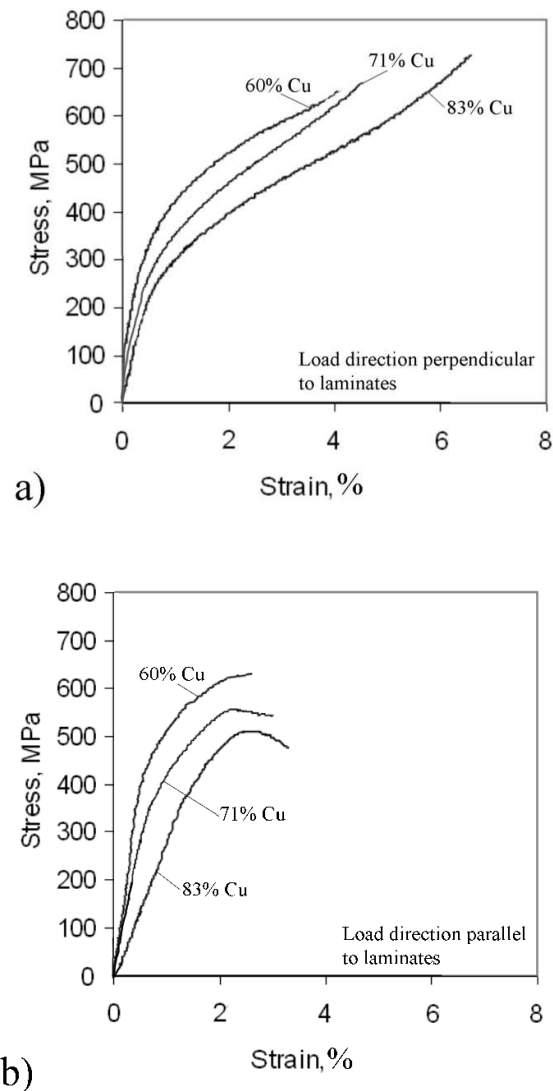


Fig. 2. Stress-strain curves at different loading directions

3. Results and discussion

3.1. Quasi-static compression tests

A large number of compression tests were performed on metal-intermetallic laminated composites. Rohatgi et al. [23] and Li et al. [45] have discussed the mechanisms of damage evolution and worked out several models of crack propagation. The tested samples were characterised in order to understand damage evolution as a function of volume fraction of unreacted copper and of the compressive loading direction, perpendicular and parallel to the laminate planes. Since the specimens were tested under the same conditions, the volume fraction of copper was thought to be a key factor in explaining the difference of failure mode. Figures 3(a) and (b) show the quasi-static stress-strain curves of specimens for different volume fractions of copper (60%, 71% and 83%) at different load directions during a compression test.

The copper-intermetallic composite has about 50% higher strength in parallel compression than in perpendicular compression (609 MPa and 414 MPa for 60% volume fraction of copper, 556 MPa and 385 MPa for 71% volume fraction of copper, 518 MPa and 332 MPa for 83% volume fraction of copper, respectively). Fig. 3 shows the typical pictures of copper-intermetallic composites after quasi-static loading in parallel direction.

The principal features are parallel cracks propagating along the layers of intermetallic phases and buckling of the copper layers. These parallel cracks run in the centre of the intermetallics, along a plane with greater defects. This is a residue from synthesis stage and impurities are segregated along the centre plane (Fig. 4).

When the intermetallic layers fail, the copper layers take the additional loading and have the tendency to buckle (Figures 3b and 5).

The composites have fewer tendencies for buckling with decreasing volume fraction of copper. Since the composites with 60% volume fraction of copper are the stiffest they fail by catastrophic cracking both of intermetallic layers and copper layers. The cracks are inclined ($30\div 45^\circ$) to the interface and initiate the formation of shear bands in the copper layers, leading to shear failure (Figures 3c and 6).

Deformation due to shear band formation was reported also in earlier papers [20, 23, 45]. The authors stated that shear deformation was initiated by cracking in the brittle layers of the composites.

Figure 7 shows the picture of the copper-intermetallic composite (71% volume fraction of copper) after quasi-static loading in perpendicular direction.

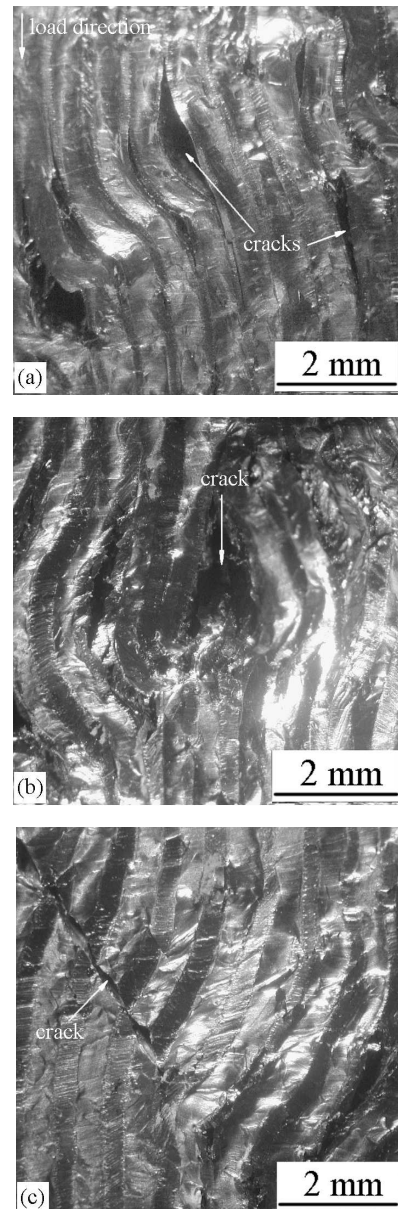


Fig. 3. Optical micrographs of tested composites after compression in parallel loading: (a) 83% Cu, (b) 71% Cu and (c) 60% Cu

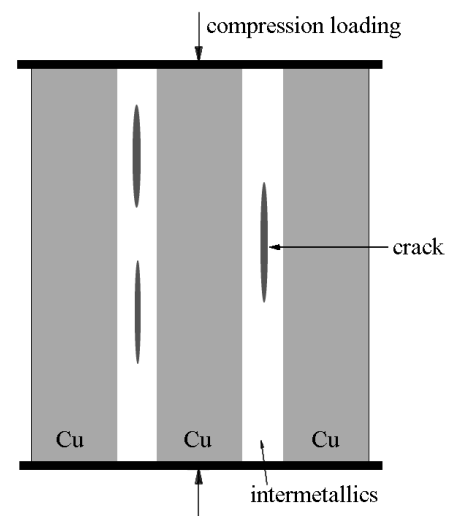


Fig. 4. Axial splitting along central plane of intermetallics layer

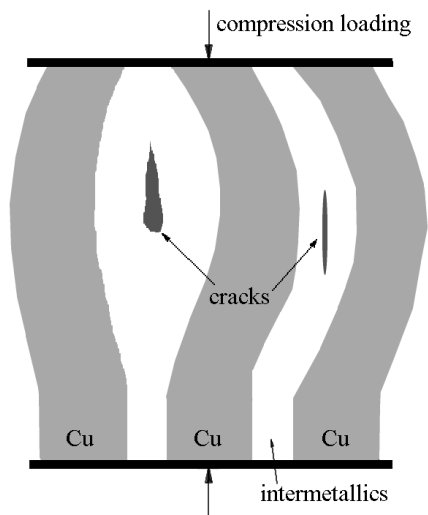


Fig. 5. Plastic buckling of copper layers during compression in parallel loading

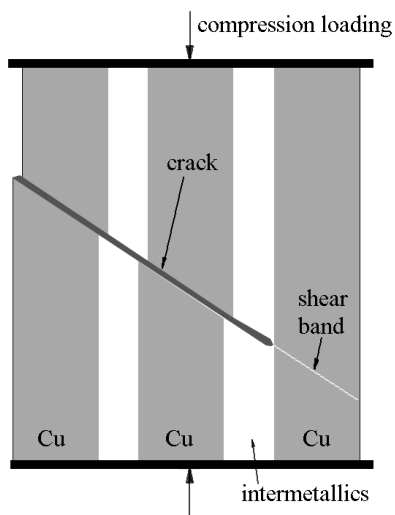


Fig. 6. Inclined cracks propagation during compression in parallel loading

Damage initiates by the formation of axial splitting cracks in the intermetallic. These cracks are limited in size by the thickness of intermetallic layer and connected via shear bands in the copper layer with the cracks in adjacent layers (Fig. 8).

Now the plastic flow takes place in the copper layers is restricted to the small regions between opposite cracks in the neighbouring intermetallic layers and it leads to the final failure of the laminated composite.

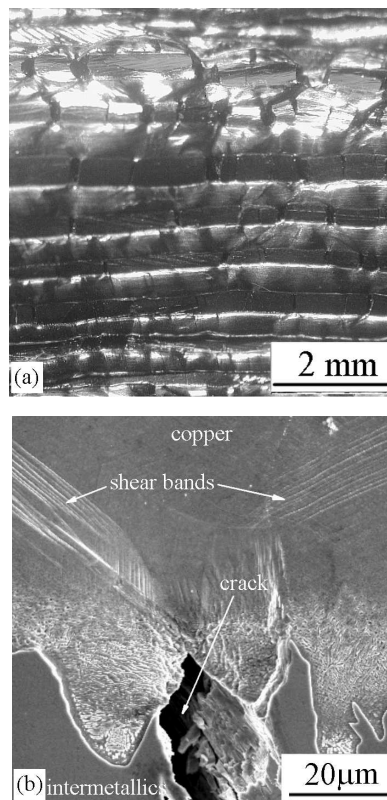


Fig. 7. Microstructure of the copper-intermetallic composite after compression in perpendicular loading: (a) topography of the specimen, (b) SEM micrograph showing crack in intermetallic layer and shear bands in copper

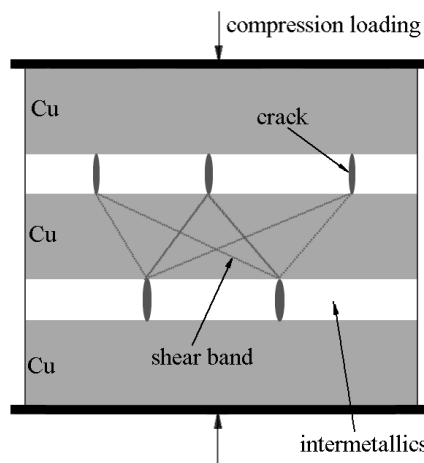


Fig. 8. Propagation of cracks and shear bands during compression in perpendicular loading

3.2. Impact tests

For the impact toughness measurements, two loading directions were used: one in perpendicular and another parallel to the laminates. Also two types of specimens with different notch configuration were prepared in the edge- and face-orientations (Fig. 9).

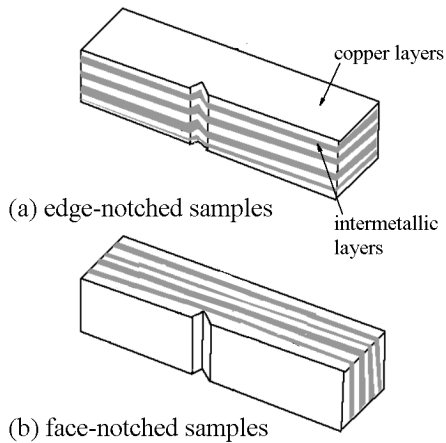


Fig. 9. Schematic representation of sample geometry to study crack propagation in copper-intermetallic laminates during impact test

TABLE 3

The impact toughness of laminated copper-intermetallic composites under different testing conditions

Volume fraction of unreacted copper in composite, %	Impact toughness, J/cm ²	
	Edge-notched samples	Face-notched samples
60	18.4	36.6
71	20.8	47.1
83	27.0	63.8

Results of impact toughness measurements are listed in Table 3. It can be found that these composites exhibit anisotropic mechanical properties. When the load perpendicular to the laminates is applied, the composites display superior impact toughness. Furthermore, it increases with increasing volume fraction of unreacted copper thickness.

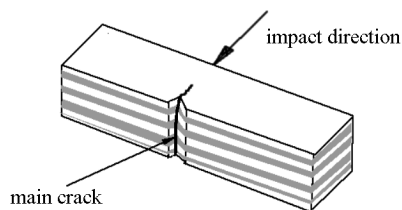


Fig. 10. Crack propagation in edge-notched sample

Figure 10 shows schematic diagram of damage evolution of the edge-notched sample. The failure occurred by cleavage mode showing limited plastic deformation.

Therefore, it is evident that there is solely one main crack parallel to the initial notch direction. The crack initiates from some surface defects, grows gradually in the through-thickness direction and finally travels across the sample.

As shown in Fig. 11, the damage evolution of face-notched samples was unlike. A crack initiated in the intermetallic layer from surface defects did not travel across the specimen, but was arrested and deflected by the adjacent copper layer. Further loading causes the formation of some new cracks in the next intermetallic layer. As a result a plastic strain of copper is localised in shear bands between opposite cracks. This process is repeated until all the intermetallic layers have cracked resulting in tortuous crack propagation patch. In this case, there is one main crack and several branching smaller cracks. The failure occurred by cleavage mode showing extensive plastic deformation.

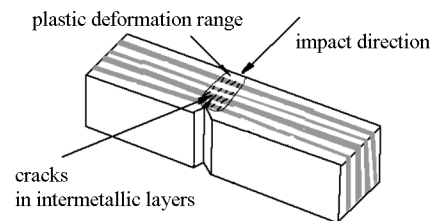


Fig. 11. Crack propagation in face-notched sample

It should be added that delamination or debonding of layers has been shown in the literature to be detrimental to the performance of laminated composites [45, 47], but these failure mechanisms were not observed in any of the samples tested. The absence of delamination of the copper and intermetallic layers during mechanical testing is an indication of the excellent bonding between the layers.

4. Conclusions

The mechanical properties and fracture behaviour of the laminated copper-intermetallic composites were examined. The following principal conclusions can be drawn:

1. The results of mechanical testing show that the composites exhibit anisotropic features.
2. The copper-intermetallic composite has about 50% higher strength in parallel compression than in perpendicular compression
3. The specimens compressed in the parallel direction failed by cracking along the middle of the intermetallic layers, buckling of copper layers and cracking inclined $30\div 45^\circ$ to the interface initiating the formation of shear bands in the copper layers.

4. The specimens compressed in the perpendicular direction failed by cracking of the intermetallic layers perpendicular to the interface and shear.
5. Impact tests show that when the load perpendicular to the laminates is applied, the composites display superior impact toughness. The toughness increases with increasing remaining Cu metal thickness.
6. The failure during impact testing occurs by cleavage mode showing limited plastic deformation for the specimens loaded parallel to the laminates and extensive plastic deformation for the specimens loaded perpendicularly.
7. No delamination or debonding of layers during tests indicates the excellent bonding between the layers.

Acknowledgements

The authors would like to thank Ms Danuta Kępka for her assistance with sample preparation.

REFERENCES

- [1] P.M. Anderson, J.F. Bingert, A. Misra, J.P. Hirth, *Acta Mater.* **51**, 6059 (2003).
- [2] S. Tixier-Boni, H. Swygenhoven, *Thin Solid Films* **342**, 188 (1999).
- [3] X.W. Zhou, H.N.G. Wadley, R.A. Johnson, D.J. Larso, N. Tabat, A. Cerezo, A.K. Pettford-Long, G.D.W. Smith, P.H. Clifton, R.L. Martens, T.F. Kelly, *Acta Mater.* **49**, 4005 (2001).
- [4] A.S. Edelstain, R.K. Everett, G.R. Richardson, S.B. Qadri, J.C. Foley, J.H. Perepezko, *Mater. Sci. Eng.* **A195**, 13 (1995).
- [5] T.S. Dyer, Z.A. Munir, *Metall. Mater. Trans.* **26B**, 603 (1995).
- [6] U. Anselmi-Tamburini, Z.A. Munir, *J. Appl. Phys.* **66**, 5039 (1989).
- [7] D.E. Alman, J.A. Hawk, A.V. Petty, J.C. Rawers, *JOM* **46**, 31 (1994).
- [8] D.E. Alman, C.P. Dogan, J.A. Hawk, J.C. Rawers, *Mat. Sci. Eng. A* **192-193**, 624 (1995).
- [9] P. Zhu, J.M.C. Li, C.T. Liu, *Mat. Sci. Eng.* **A239-240**, 532 (1997).
- [10] Z. Xia, J. Liu, S. Zhu, Y. Zhao, *J. Mater. Sci.* **34**, 3731 (1999).
- [11] L. Battezzati, P. Pappaleopore, F. Durbiano, I. Gallino, *Acta Mater.* **47**, 1901 (1999).
- [12] R. Banerjee, J.P. Fain, P.M. Anderson, H.L. Fraser, *Scripta Mater.* **44**, 2629 (2001).
- [13] K.J. Blobaum, D. Van Heerden, A.J. Gavens, T.P. Weihs, *Acta Mater.* **51**, 3871 (2003).
- [14] H. Takuda, H. Fujimoto, N. Hatta, *J. Mat. Sci.* **33**, 91 (1998).
- [15] N. Masahashi, K. Komatsu, G. Kimura, S. Watanabe, S. Hanada, *Metall. Mater. Trans.* **37A**, 1665 (2006).
- [16] N. Masahashi, M. Oku, S. Watanabe, S. Hanada, *Mater. Sci. Forum* **539-543**, 866 (2007).
- [17] H. Cao, J.P.A. Lofvander, A.G. Evans, R.G. Rowe, D.W. Skelly, *Mat. Sci. Eng.* **A185**, 87 (1994).
- [18] D.R. Bloyer, K.T. Venkateswara Rao, R.O. Ritchie, *Mat. Sci. Eng.* **A216**, 80 (1996).
- [19] D.R. Bloyer, K.T. Venkateswara Rao, R.O. Ritchie, *Mat. Sci. Eng.* **A239-240**, 393 (1997).
- [20] D.R. Bloyer, K.T. Venkateswara Rao, R. Ritchie, *Metallurgical Trans.* **29A**, 2483 (1998).
- [21] D.S. Chung, M. Enoki, T. Kishi, *Sci. Technol. Adv. Mater.* **3**, 129 (2002).
- [22] R. Mola, A. Dziadoń, In: *Proceedings of the 6-th European Conference of Young Research and Science Workers TRANSCOM*, Zilina, Slovak Republic 81 (2005).
- [23] A. Rohatgi, D. Harach, K.S. Vecchio, K. Harvey, *Acta Mater.* **51**, 2933 (2003).
- [24] J.G. Luo, V.L. Acoff, *Mat. Sci. Eng.* **A379**, 164 (2004).
- [25] K.S. Vecchio, *JOM* **57**, 25 (2005).
- [26] R.R. Adharapurapu, K.S. Vecchio, F. Jiang, A. Rohatgi, *Metall. Mater. Trans.* **36A**, 1595 (2005).
- [27] L.M. Peng, J.H. Wang, H. Li, J.H. Zhao, L.H. He, *Scripta Mater.* **52**, 243 (2005).
- [28] D. Chung, J. Kim, M. Enoki, *Mater. Sci. Forum* **475-479**, 1521 (2005).
- [29] T. Li, J. Fenghun, E.A. Olevsky, K.S. Vecchio, M.A. Meyers, *Mat. Sci. Eng.* **A443**, 1 (2007).
- [30] D. Harach, K.S. Vecchio, *Metall. Mater. Trans.* **32A**, 1493 (2001).
- [31] M. Konieczny, A. Dziadoń, *Inżynieria Materiałowa* **6**, 639 (2003).
- [32] A. Dziadoń, M. Konieczny, *Kovové Mater.* **42**, 42 (2004).
- [33] M. Konieczny, A. Dziadoń, *Mat. Sci. Eng.* **A460-461**, 238 (2007).
- [34] M. Konieczny, *Kovové Mater.* (2007) in press.
- [35] L. Xian, Y. Yanqing, M. Yungwang, H. Bin, Y. Meini, C. Yan, *Scripta Mater.* **56**, 569 (2007).
- [36] H.C. Cao, A.G. Evans, *Acta Metall. Mater.* **39**, 2997 (1991).
- [37] M.C. Shaw, D.B. Marshall, M.S. Dadkhah, A.G. Evans, *Acta Metall. Mater.* **41**, 3311 (1993).
- [38] D.E. Alman, J.C. Rawers, J.A. Hawk, *Metallurgical Trans.* **26A**, 589 (1995).
- [39] J.C. Rawers, K. Perry, *J. Mat. Sci.* **31**, 3501 (1996).
- [40] J.C. Rawers, D.E. Alman, *Compos. Sci. Technol.* **54**, 379 (1995).
- [41] F.G. Buchholz, R. Rikards, A. Wang, *Int. Journal of Fracture* **86**, 37 (1997).
- [42] W. Wenchao, R. Singh, *Mat. Sci. Eng.* **A271**, 306 (1999).
- [43] M. Li, W.O. Soboyejo, *Metallurgical Trans.* **31A**, 1385 (2000).

- [44] N. Rudnitskii, *Strength of Materials* **34**, 612 (2002).
- [45] T. Li, F. Grignon, D.J. Benson, K.S. Vecchio, E.A. Olevsky, J. Fenghun, A. Rohatgi, R.B. Schwarz, M.A. Meyers, *Mat. Sci. Eng.* **A374**, 10 (2004).
- [46] H. Wang, J. Han, S. Du, D. Northwood, *Metall. Mater. Trans.* **38A**, 409 (2007).
- [47] G.R. Odette, B.L. Chao, J.W. Sheckherd, G.E. Lucas, *Acta Metall. Mater.* **40**, 2381 (1992).

Received: 10 February 2007.